Composites: Part B xxx (2014) xxx–xxx

Contents lists available at ScienceDirect

Composites: Part B

journal homepage: www.elsevier.com/locate/compositesb

Defect localization based on modulated photothermal local approach

Bertrand Lascoup [a], Laetitia Perez [b], Laurent Autrique [c,*]

[a] IRT Jules Verne, Chemin du Chaffault, 44340 Bouguenais, France
[b] Laboratoire de Thermocinétique de Nantes – UMR CNRS 6607, rue Christian Pauc, 44306 Nantes Cedex 03, France
[c] Université d'Angers, 62 Avenue Notre Dame du Lac, 49000 Angers, France

ARTICLE INFO

Article history:
Received 5 June 2013
Received in revised form 27 November 2013
Accepted 12 December 2013
Available online xxxx

Keywords:
D. Non destructive testing
B. Defects
Modulated photothermal method

ABSTRACT

A new method dedicated to macroscopic-like defect localization in composite materials is presented in this paper. The proposed method is based on non intrusive measurements of the sample temperature resulting from a local periodic low energy heating. In such an approach, the low temperature increases of the investigated material avoid damages which can occur with usual flash techniques. Since thermal waves propagation is modified due to the heterogeneity induced by the defect, analysis of both modulus and phase lag spatial distributions provides relevant knowledge. Up to now, macroscopic-like defect detection based on local periodic heating has not been widely investigated. Thus, differences between the global approach and the local approach have to be pointed out in order to verify the local method's attractiveness. A mathematical model based on complex temperature is developed and provides a relevant predictive tool. In several configurations interest of local periodic heating is highlighted. For example, while several defects are included in the sample, the method capability to distinguish one from each other is shown considering a scanning approach. In order to validate these results, an experimental device has been developed. Several non destructive inspections are performed and defect detection is achieved using an infra-red camera providing observations of the sample surface.

1. Introduction

An accurate inspection of structural material properties combined with relevant structural health monitoring (SHM) is nowadays required to guarantee the quality of any structure. In such an aim, defect embedded in a composite structure can be localized and analyzed using acoustic techniques. Unfortunately for such techniques (C-SCAN for example [1]) a fluid vector is usually required and can damage the investigated material. In order to avoid sample contamination, a non-destructive approach based on thermal observations of the sample surface using an infra-red camera can enable defects detection; see for example [2] for crack detection at micrometric scale, [3,4] for recent applications. More specifically, the active thermography method proposed in [3] is the step heating and consists in sample heating for a given time length (ranged between 60 s and up to 1 h). Then thermal observations are considered during the whole relaxation process. Main drawbacks of this approach is to potentially induce high temperature and modifies (or damages) the investigated structure. Another thermal testing is based on modulated heating which allows small relevant temperature oscillations (induced by a low periodic heating). Propagation of low energetic thermal waves in samples has been investigated in [5–7]. Several applications devoted to parametric identification are presented in [8–10] for millimetre scale and in [11,12] for micrometric investigation. Modulated thermal heating have been recently carried out for macroscopic-like defect detection. A quite original application is proposed in [13]: a mural paint (XIVth century) is examined before its possible restoration (non-destructive techniques is obviously a key requirement). One can refer to [14,15] for other examples dedicated to composite non-destructive inspection. In [16], fatigue cracks in steel bridges are investigated. Usually, the sample is periodically heated on a surface which is quite larger than the suspected defect. Thus, such approach is devoted to the detection of a defect which is located under the heated surface. The approach proposed in the following is based on a local excitation (heated surface can be lower than the defect). Indeed, in thin plate, propagation of thermal waves from the side can be more revealing than a vertical propagation. A preliminary feasibility study has been presented in [17] and the complementary work presented in this communication is focused, on one hand, on the comparison between global and local approach and, on the other hand, on the localization of the heterogeneity modifying the thermal waves propagation.

This paper is organized as follows. First of all, partial differential equation system describing the temperature evolution in the sample is given in the specific case of periodic input. Complex

* Corresponding author. Tel.: +33 241 226 518; fax: +33 241 226 561.
E-mail addresses: bertrand.lascoup@irt-jules-verne.fr (B. Lascoup), laetitia.perez@univ-nantes.fr (L. Perez), laurent.autrique@univ-angers.fr (L. Autrique).

1359-8368/$ - see front matter © 2013 Elsevier Ltd. All rights reserved.
http://dx.doi.org/10.1016/j.compositesb.2013.12.012

temperature is introduced in order to avoid consuming computational time. Principle of periodic method is briefly exposed and the mathematical model satisfied by temperature expressed in its complex formalism is presented. Numerical resolution based on finite element method is performed and both global and local approaches are investigated in order to illustrate the defect effect on both modulus and phase lag spatial distributions. Then several configurations are considered and assess the method attractiveness.

2. Mathematical model

2.1. State equations

Let us consider that the periodic heating flux can be expressed without lack of generalities as follows:

$$\Phi(x,y,z;t) = \phi_0(x,y,z)\cos(\omega t) \tag{1}$$

where $(x,y,z) \in \Omega \subset \mathbb{R}^3$ is the space variable, t is the time variable, $\phi_0\,(x,y,z)$ is constant on a disk (radius R on the heated sample surface $\Gamma_0 \subset \partial\Omega$), ω is the pulsation in (rad s^{-1}). For a realistic periodic signal, $\Phi(x,y,z;t)$ is the first harmonic. Temperature evolution for each sample point tends towards a periodic state after a transient one. Such oscillations are completely defined by their amplitude $|T(x,y,z)|$ (also called modulus) and their phase lag $\varphi(x,y,z)$ when compared with a reference signal (heating input for example). Let us introduce the complex notation $\widetilde{T}(x,y,z) = |T(.)|\exp(j\phi(.))$ solution of the following partial differential equations system (see for example [8,9,18,19]):

$$\forall(x,y,z) \in \Omega \quad \widetilde{T}(x,y,z) + \frac{j}{\omega}\mathrm{div}(\vec{\vec{\alpha}}\ \overline{\mathrm{grad}\ \widetilde{T}(x,y,z)}) = 0 \tag{2}$$

$$\forall(x,y,z) \in \Gamma_0 \quad -\lambda \Rightarrow \frac{\partial\widetilde{T}(x,y,z)}{\partial\vec{n}} = h\widetilde{T}(x,y,z) - \phi_0 \tag{3}$$

$$\forall(x,y,z) \in (\partial\Omega/\Gamma_0) \quad -\lambda \Rightarrow \frac{\partial\widetilde{T}(x,y,z)}{\partial\vec{n}} = h\widetilde{T}(x,y,z) \tag{4}$$

where $\vec{\vec{\alpha}} = \frac{\vec{\vec{\lambda}}}{C}$ is the thermal diffusivity tensor in (m^2 s^{-1}), $\vec{\vec{\lambda}}$ is the thermal conductivity tensor in (W m^{-1} K^{-1}), C is the volumetric heat in (J m^{-3} K^{-1}), $\vec{n}$ is the unit vector external outward-pointing normal to $\partial\Omega$, h is the convective heat transfer coefficient in (W m^{-2} K^{-1}).

For an isotropic material, at a given frequency $f = \frac{\omega}{2\pi}$ diffusion length defined as $\mu = \sqrt{\frac{\alpha}{\pi f}}$ in (m) is a key parameter for periodic methods. In fact, in thermal sciences, it is usually considered that effect of thermal wave vanishes at distance greater than 3μ from the heating excitation. In the context of experimental investigations, frequency has to be carefully adapted to the sample size. In the following several configurations are studied in order to illustrate the differences between the global approach (corresponding to a large disk radius) versus the local one (corresponding to a small disk radius). "Large" and "small" radius are defined according to the sample geometry (thickness, ...) and the defect size.

2.2. Transmission

In this section, direct problem (2–4) is solved using finite element method and Comsol® software (see [20–24]). A semi infinite thin plate (thickness e = 5 mm) is considered. Thermo physical parameters corresponding to a Teflon (also called PTFE for Polytetrafluoroethylene) sample are presented in Table 1. Let us consider that observations are performed by an infrared camera on the opposite face than the heated one; such configuration is called transmission. Both modulus (temperature oscillations amplitude) and phase lag are investigated on the non heated face. If the modulus is too attenuated, phase lag analysis is meaningless. Then, for each point of the heating surface, if $|T(x,y,z)| \leqslant 0.01\max_{\Gamma_0}|T|$ then $\varphi(x,y,z) = -150°$.

A small aluminum disk (1 cm radius, 1 mm thickness) is located inside the previous PTFE sample. Defect thermal diffusivity is $\alpha_{def} = 6.5\ \ 10^{-5}$ (m^2 s^{-1}) while defect thermal conductivity is $\lambda_{def} = 160$ (W m^{-1} K^{-1}). This defect is located at a distance of 2 cm from the PTFE plate center. Two approaches are compared. For the first one, heating disk radius is greater than the plate size in order to heat the whole PTFE surface. This first approach is called in the following "global approach". For the second approach, a smaller heating disk radius is taken into account R = 1 cm in order to provide a local heating (in the centre of the heated face). A coarse mesh is considered: 4806 nodes and 19,633 quadratic Lagrange-type tetrahedral elements. The following figures are proposed in order to illustrate the differences between global and local approaches (excitation frequency is $f = 0.001$ Hz):

- Fig. 1: oscillations modulus (amplitude) for both global and local approaches. Spatial distribution of $|T(x,y,z)|$ are drawn for $R = \infty$ (global) and for R = 1 cm (local). Modulus range for global heating is [4.7, 13.1] while for local heating modulus range is [0, 5.4].
- Fig. 2: modulus comparison with material without defect (for both approaches). Spatial distribution are compared without defect $|T(x,y,z)|_{ref}$ and with defect $|T(x,y,z)|_{def}$ and the following distribution is drawn:

$$\frac{|T(x,y,z)|_{def} - |T(x,y,z)|_{ref}}{\max(||T(x,y,z)|_{def} - |T(x,y,z)|_{ref}|)} \tag{5}$$

Such distribution is called reduced contrast. "Contrast" means that it takes into account the difference between the modulus distributions obtained with the defected sample and with the sample without defect. "Reduced" means that contrast is normalized in order to be compared with other configurations. Modulus reduced contrast range for global heating is [0.15, 1] while for local heating reduced contrast range is [−1, 0.41]. Effect of defect on thermal waves propagation is highlighted for the local approach.

- Fig. 3: phase lag for both global and local approaches. Phase lag range for global heating is [−0.5, 74.5] while for local heating phase lag range is [−160, 0.6]. Unit is degree of arc denoted by °.
- Fig. 4: phase lag comparisons with material without defect (for both approaches). The following spatial distribution is plotted: $\frac{\phi_{def}(x,y,z) - \phi_{ref}(x,y,z)}{\max(|\phi_{def}(x,y,z) - \phi_{ref}(x,y,z)|)}$. Phase lag reduced contrast range for global heating is [−0.05, 1] while for local heating reduced contrast range is [−0.15, 1]. Effect of defect on thermal waves propagation is highlighted for the local approach.

Considering these figures, it is shown that global approach is not as sensitive as the local one. Moreover, the defect location

Table 1
Thermophysical parameter (PTFE sample).

Diffusivity (m^2 s^{-1})	Conductivity (W m^{-1} K^{-1})	Convective coefficient (W m^{-2} K^{-1})	Heating flux (W m^{-2})
$\alpha = 1.035 \times 10^{-7}$	$\lambda = 0.24$	$h = 7.5$	$\Phi_0 = 5 \times 10^2$

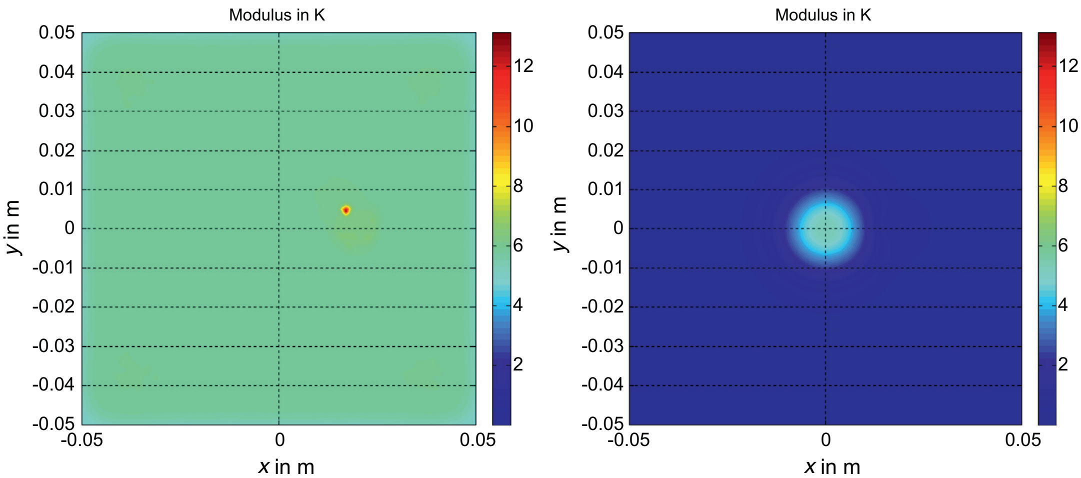

Fig. 1. Simulated modulus for global (left) and local (right) approaches.

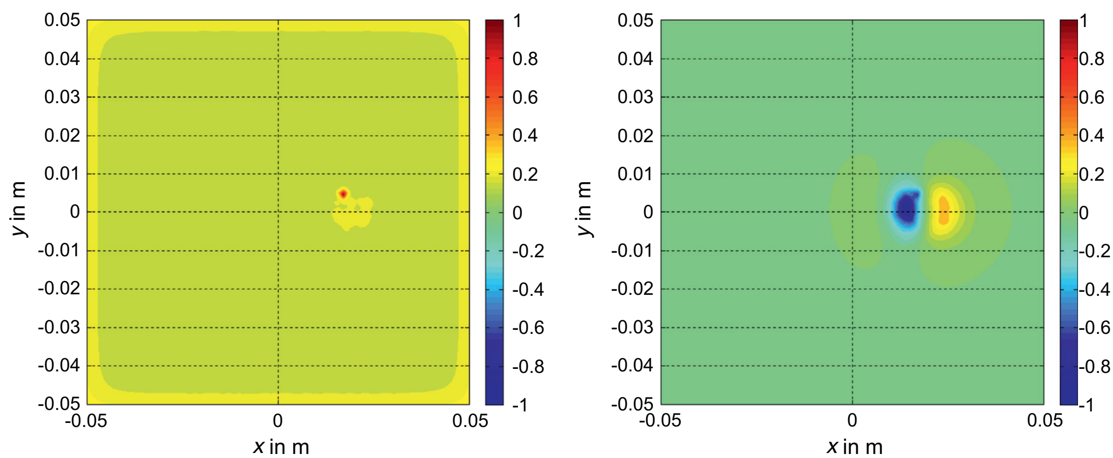

Fig. 2. Reduced contrast for modulus: global (left) and local (right) approaches.

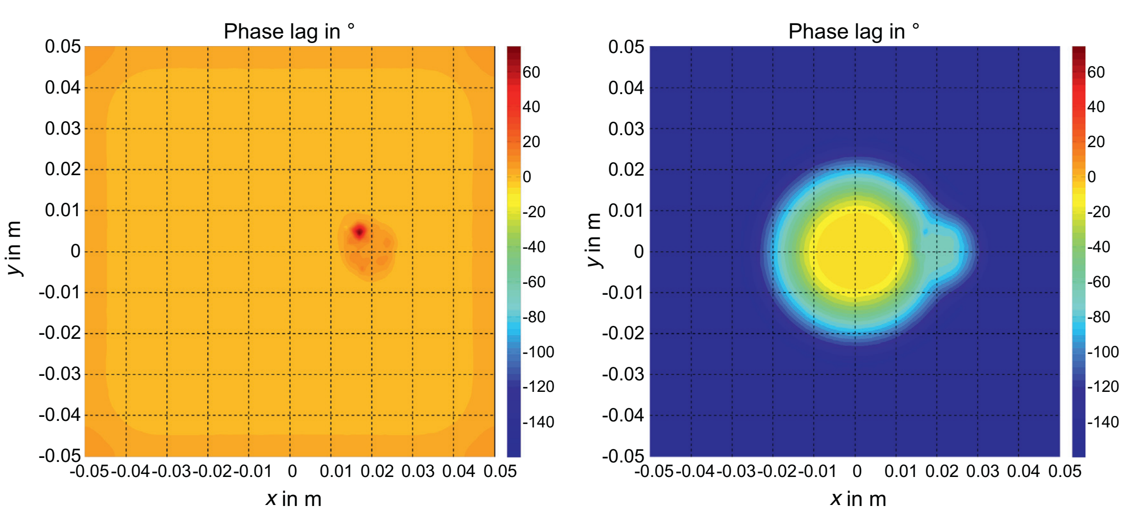

Fig. 3. Simulated phase lag for global (left) and local (right) approaches.

can be deduced considering modulus contrast. Phase lag contrast for a local heating is more difficult to analyze for defect localization. In order to illustrate that a refined mesh is useless, modulus reduced contrast is drawn considering 42,451 nodes and 203,138 elements (see Fig. 5). Comparisons between Figs. 2 and 5 shows that a refined mesh is not more informative about defect effect

Please cite this article in press as: Lascoup B et al. Defect localization based on modulated photothermal local approach. Composites: Part B (2014), http://dx.doi.org/10.1016/j.compositesb.2013.12.012

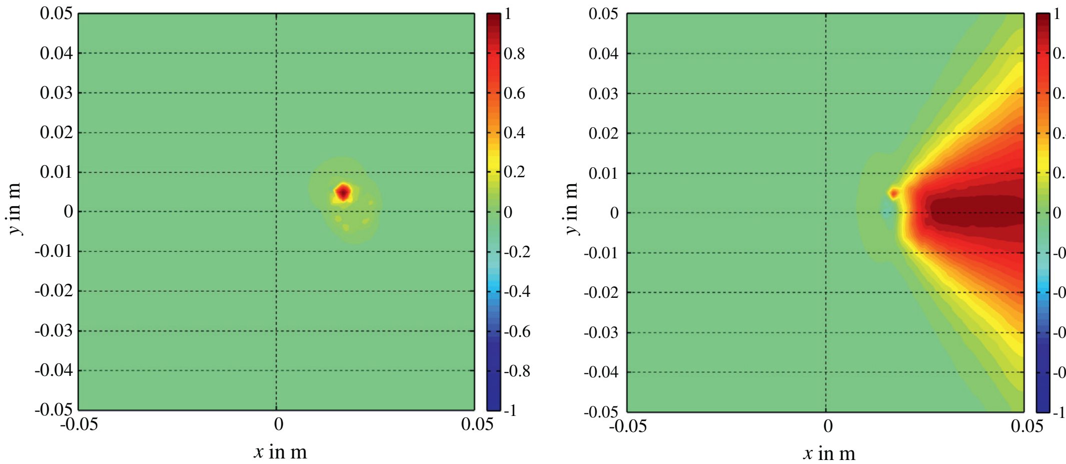

Fig. 4. Reduced contrast for phase lag: global (left) and local (right) approaches.

on thermal wave propagation and that defect location can be estimated considering results obtained with coarse mesh. In the next section, detection of a fibers misalignment is performed in reflection configuration.

2.3. Reflection

In reflection, temperature oscillations are observed on the sample heated face. Heating disk radius is equal to 5 mm and heat flux is 10^5 ($\mathrm{W\,m^{-2}}$). Natural convection coefficient is $h = 7.5$ [$\mathrm{W\,m^{-2}\,K^{-1}}$]. An orthotropic material is investigated (3 mm thick plate). The 3 mm thick defect corresponds to a disk (radius 5 mm) inducing a fibers misalignment (angle is $\beta_i = 10i$ in degree for $i = 1, \cdots, 9$). The defect centre is located at the point (10, 10, 0) (in mm). Excitation frequency is 0.005 Hz. Thermal properties of investigated material are given in Table 2. In Fig. 6, fibers misalignment effect is shown: modulus contrast are drawn for each angle $\beta_i = 10i$. In Table 3, minimum contrast and maximum contrast are given for each angle β_i. Considering these results, it is established that thermal waves propagation is significantly affected by such defect. Thus, fibers misalignment can be easily detected and localized by analyzing modulus differences in reflection.

In the following section, defect localization is investigated.

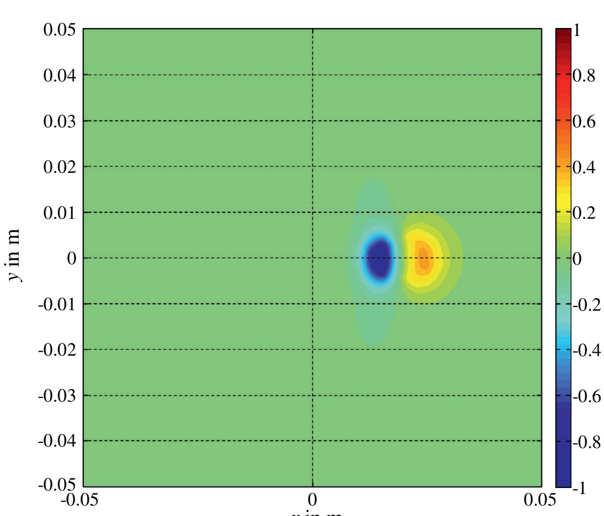

Fig. 5. Reduced contrast for modulus considering a refined mesh.

3. Defect localization based on scanning approach

3.1. Scanning approach

Due to the quite low diffusion length, the distance between defect and heating area can be too important to ensure a proper detection (and localization). Thus, development of a scanning approach is required in order to investigate realistic experimentations. Several measurements are performed on the heated sample surface. In the studied configuration, the heating point is moving around the defect (a grid corresponding to eight locations is proposed in Fig. 7). The investigated sample is a plate with dimension quite larger than the area heated by the modulated heating source. Considering the studied configuration, thermal diffusion length is $\mu = \sqrt{\frac{\alpha}{\pi f}} \approx 5.7$ mm. Thus at a distance greater than $3\mu \approx 1.7$ cm from the heating excitation, it is usually considered that effect of thermal wave vanishes. Thus the PTFE sample can be considered as a semi-infinite plate. Each experimentation leads to a modulus spatial distribution and the following results are proposed:

- Fig. 8: this example is obtained with a defect (aluminum disk: 5 mm radius, 1 mm thickness) located at the sample center. The studied sample is a PTFE square plate (thickness 5 mm). Heating disk radius is $R = 5$ mm; frequency is $f = 0.001$ Hz; heat flux is 5 $\mathrm{kW\,m^{-2}}$. Modulus contrasts ($|T(x,y,z)|_{def} - |T(x,y,z)|_{ref}$) are drawn for each heating disk location. Range is in $[-10.5, 3.5]$.
- Fig. 9: sum of the eight spatial distributions presented in Fig. 8.

Analysis of previous figures leads to a correct defect localization.

3.2. Localization of twin defects using scanning approach

In this section, two similar defects are considered (aluminum disk presented in previous section). In Fig. 10, results issued from the sum of the eight scanning are presented for several distances between each defect (disk center): 1 cm, 2 cm and 3 cm. In this figure, effect of distance between defects centers is pointed out. The proposed method is able to highlight the number of defect. When the distance between the two defects is equal to 3 cm, the scanning approach (successive modulated heating on a grid defined in Fig. 7) shows the location of the two disk centers: -1.5 cm and +1.5 cm. When the distance between the two disk defects is reduced, it is more difficult to accurately define the centers location. This is

Table 2
Thermal parameters for fiber misalignment detection.

	Orthotropic material	Patch: disk $D_{i=1,\cdots,9}\beta = i\frac{\pi}{18}$
Thermal conductivity λ (W m^{-1} K^{-1})	$\begin{bmatrix} 1 & 0 & 0 \\ 0 & 5 & 0 \\ 0 & 0 & 1 \end{bmatrix}$	$\begin{bmatrix} 1+4\sin\beta & 0 & 0 \\ 0 & 1+4\cos\beta & 0 \\ 0 & 0 & 1 \end{bmatrix}$
Volumetric heat capacity C (J m^{-3} K^{-1})	1.6×10^6	1.6×10^6

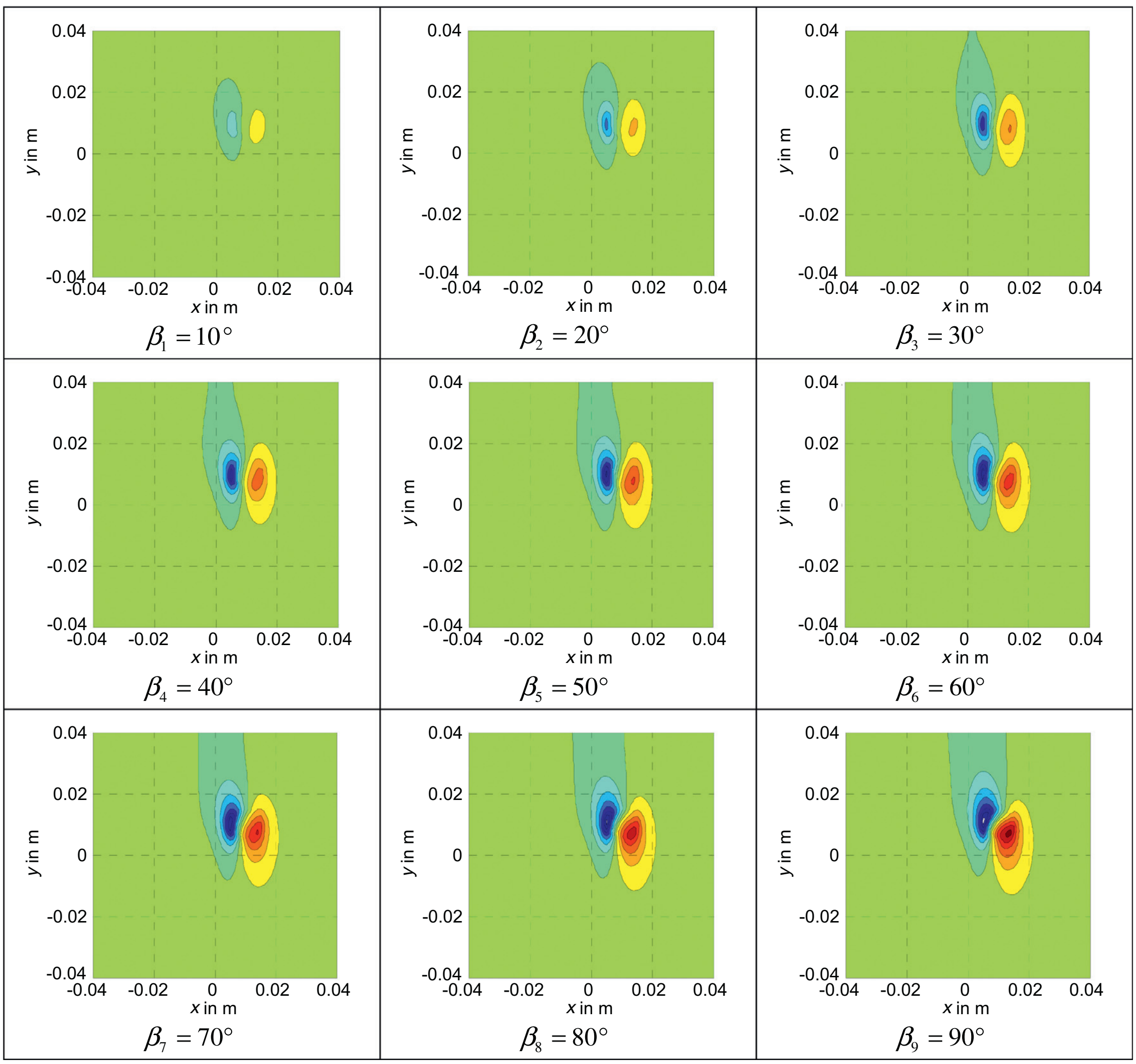

Fig. 6. Effect of fibers misalignment ($\beta \in [10°, 90°]$): modulus contrast are drawn in [−14.5, 11.5] K.

Table 3
Modulus contrast (in K).

Angle β_i	10°	20°	30°	40°	50°	60°	70°	80°	90°
Minimum	−4.2	−7.2	−9.4	−11.1	−12.2	−13.0	−13.5	−14.0	−14.3
Maximum	2.3	4.0	5.4	6.6	7.6	8.4	9.3	10.2	11.4

due to the thermal diffusion length which is the key-parameter for the spatial distribution of the modulus. In the studied configuration, $\mu \approx 5.7$ mm and in order to obtain a better localization, it is quite easy to reduce μ: if the frequency is multiplied by four, the thermal diffusion length is divided by two. In the following section, an experimental device is discussed.

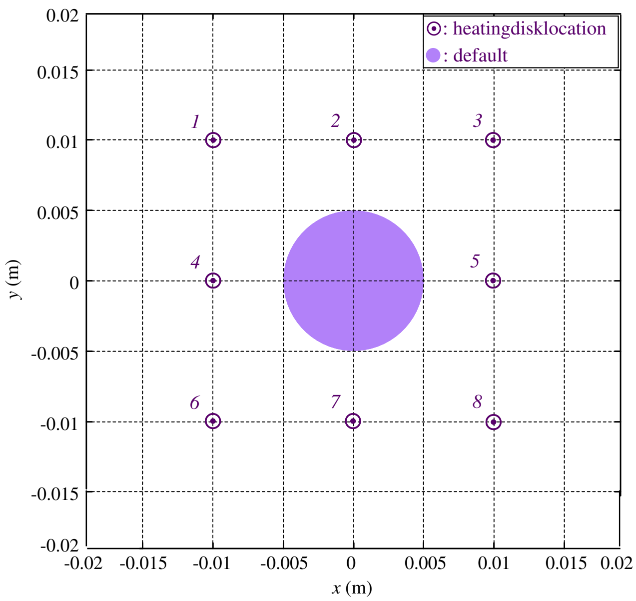

Fig. 7. Heating source locations.

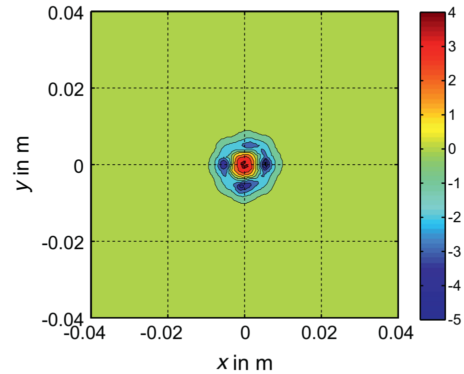

Fig. 9. Sum of the eight modulus contrasts.

3.3. Experimental validation

The experimental specific device developed in [9,17] is used (excitation frequency $f = 0.0026$ Hz) for a 50×50 mm^2 glass/polyester sample. Twin aluminum defects (1 mm thick, radius 5 mm and 15 mm between defects centers) are investigated. Results of

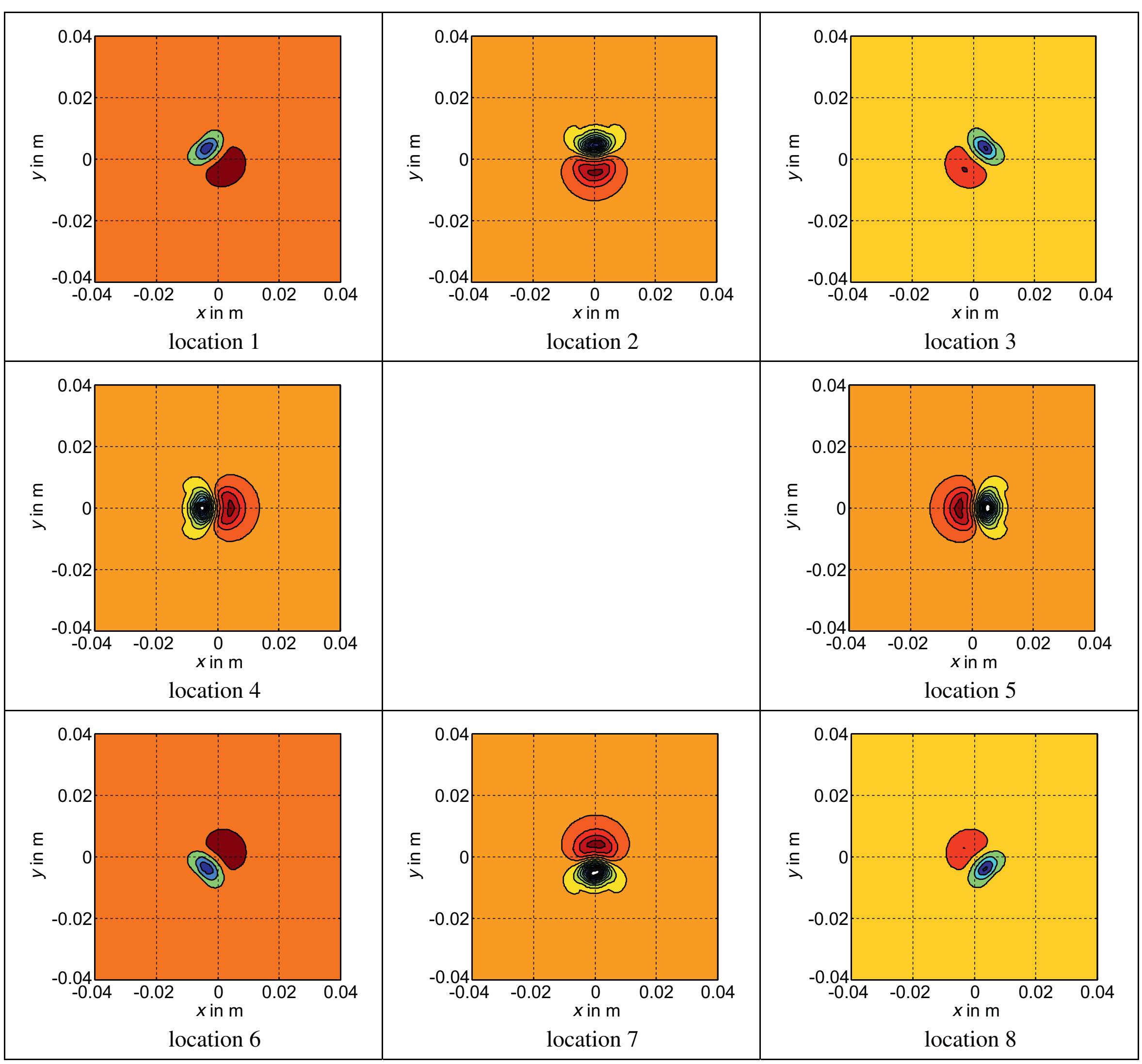

Fig. 8. Modulus contrasts (in K) for the eight heating source locations (range is [−10.5, 3.5]).

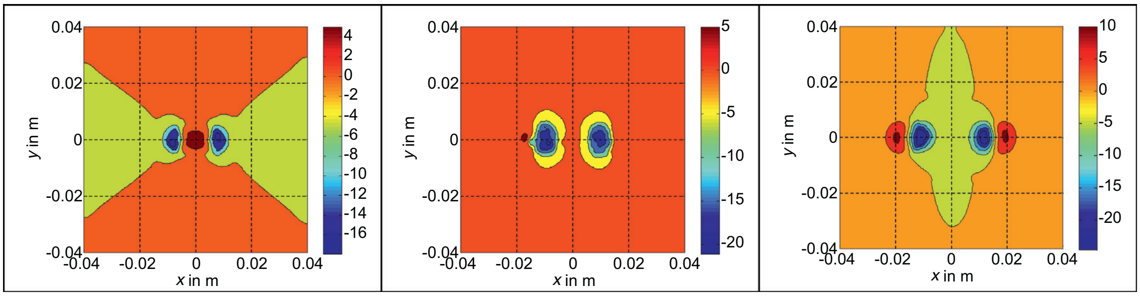

Fig. 10. Twin defects localization (sum of modulus contrasts) for several distances between defect centre: 1 cm (left), 2 cm (middle), 3 cm (right).

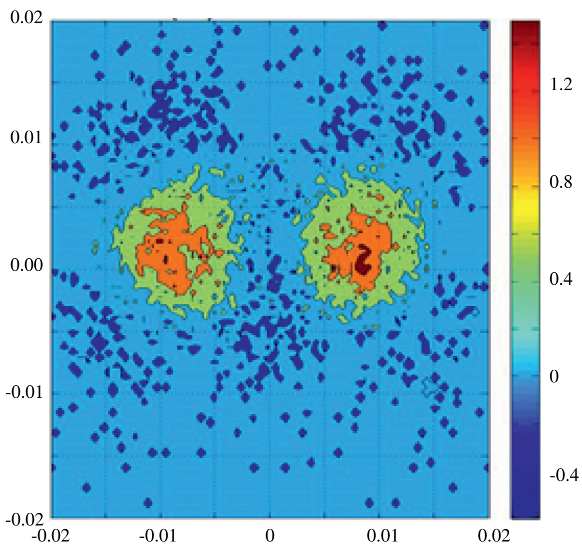

Fig. 11. Experimental results in K (sum of eight modulus contrast).

the previous scanning approach are shown in Fig. 11. It is shown that not only the twin defects can be discriminated but also that both location and defect shape can be detected.

4. Concluding remarks

In this paper, a non-destructive approach for macroscopic-like defect detection in composite materials based on the analysis of system state behavior (when sample is submitted to a modulated input) has been proposed. One of the main advantage of this technique is to be used even if the signal versus noise on observable output ratio is low and thus to preserve the material integrity. The local approach specificities offer an attractive alternative to more usual global approach. Effect of fiber misalignment on thermal waves propagation is observed (in reflection) in order to highlight the modulated photothermal local approach. This method allows a quite good separation of twin defects. Finally, an experimental device confirms the scanning method interest.

The proposed approach is not strictly devoted to fiber reinforced composite materials but can also be implemented for crack detection, unsticking monitoring.... From the experimental point of view, in usual situation, environmental temperature variation is not a nuisance parameter since modulated excitation lead to the analysis of relative variation. If ambient temperature variation range is of the same order of magnitude of temperature modulus (with a dynamic similar to the excitation one), thermal wave propagation is meaning less and the method would be not suitable in such a situation. The geometry of investigated composite components is not a crucial requirement except the need of an investigated heating surface with constant optical properties (such as absorptivity). Last, the method should be adapted to non-opaque materials.

Beyond the detection of a possible defect and the estimation of its position, further works will be focused on the identification of defect thermal properties and geometry (depth, shape).

References

[1] Hasiotis T, Badogiannis E, Tsouvalis NG. Application of ultrasonic C-scan techniques for tracing defects in laminated composite materials. J Mech Eng 2011;57–3:192–203.
[2] Bodnar JL, Egee M, Menu C, Besnard R, Le Blanc A, Pigeon M, et al. Cracks detection by a moving photothermal probe. J Phys IV 1994 [C7-4, juillet].
[3] Dumoulin J, Ibos L, Ibarra-Castanedo C, Mazioud A, Marchetti M, Maldague X, et al. Active infrared thermography applied to defect detection and characterization on asphalt pavement samples: comparison between experiments and numerical simulations. J Mod Opt 2010;57–18:1759–69.
[4] Maillard S, Cadith J, Bouteille P, Legros G, Bodnar JL, Detalle V. Non-destructive testing of forged metallic materials by active infrared thermography. Int J Thermophys 2012;33–10:1982–8.
[5] Gonzalez de la Cruz G, Gurevich YG. Thermal diffusion of a two layer system. Phys Rev B 1995;51:2188–92.
[6] Gonzalez de la Cruz G, Gurevich YG. Physical interpretation of thermal waves in photothermal experiments. Rev Mex Fis 1999;45–1:41–6.
[7] Gurevich YG, Logvinov G, Lashkevich I. Boundary conditions in theory of photothermal processes in solid. Rev Sci Instrum 2003;74–1:589–91.
[8] Perez L, Autrique L. Robust determination of thermal diffusivity values from periodic heating data. Inverse Probl IOP J 2009;25–4:45011–31.
[9] Autrique L, Perez L, Scheer E. On the use of periodic photothermal methods for materials diagnosis. Sensors Actuators B 2009;135–2:478–87.
[10] Perez L, Autrique L. Feasibility study and optimal design of an experimental bench for identification of liquids thermal diffusivity. IEEE Trans Instrum Meas 2012;61–10:2739–48.
[11] Autrique L, Perez L, Serra JJ. Finite element modelling for microscale thermal investigations using photothermal microscopy data inversion. Meas Sci Technol 2007;18:1–11.
[12] Serra JJ, Autrique L. Microscale thermal characterization of reinforced composites by photothermal microscopy data inversion. In: 5th international conference on inverse problems in engineering: theory and practice. Cambridge, United Kingdom; July 2005.
[13] Bodnar JL, Candore JC, Nicolas JL, Szatanik-Perrier G, Detalle V, Vallet JM. Stimulated infrared thermography applied to help restoring mural paintings. NDT E Int 2012;49:40–6.
[14] Ishikawa M, Hattal H, Habuka Y, Jinnai S, Utsunomiya S, Goto K. Pulse-phase-thermographic non-destructive testing for CRFP specimen. In: 14th European conference on composite materials. Budapest, Hungary; 7–10 June 2010.
[15] Grammatikos SA, Kordatos EZ, Barkoula NM, Matikas T, Paipetis A. Innovative non-destructive evaluation and damage characterization of composite aerostructures. In: 14th European conference on composite materials. Budapest, Hungary; 7–10 June 2010.
[16] Sakagami T, Izumi Y, Mori N, Kubo S. Development of self-reference lock-in thermography and its application to remote nondestructive inspection of fatigue cracks in steel bridges. In: 10th international conference on quantitative infrared thermography. Québec, Canada; 27–30 July 2010.
[17] Lascoup B, Perez L, Autrique L, Crinière A. On the feasibility of defect detection in composite material based on thermal periodic excitation. Composites: Part B 2013;45:1023–30.
[18] Carslaw HS, Jaeger JC. Conduction of heat in solids. Oxford: Clarendon-Press; 1959.
[19] Gurevich YG, Logvinov GN, de la Cruz GG, Lopez GE. Physics of thermal waves in homogeneous and inhomogeneous (two-layer) samples. Int J Therm Sci 2003;42:63–9.

Please cite this article in press as: Lascoup B et al. Defect localization based on modulated photothermal local approach. Composites: Part B (2014), http://dx.doi.org/10.1016/j.compositesb.2013.12.012

[20] Pepper DW, Heinrich JC. The finite element method – basic concepts and applications. Taylor & Francis, Group; 1992. p. 240.
[21] Zimmerman WBJ. Multiphysics modeling with finite element methods. World Scientific Publishing; 2006. p. 432.
[22] Edsberg L. Introduction to computation and modeling for differential equations. Wiley-Interscience; 2008. p. 256.
[23] Baker AJ. Finite elements: computational engineering sciences. Wiley; 2012. p. 288.
[24] Pryor RW. Multiphysics modeling using Comsol® v.4 – a first principles approach. Mercury Learn Inform 2012:700.